Optimal Design of Single-phase 12S-6P FEFSM Using Segmental Rotor and Non-Overlap Windings

Mohd Fairoz Omar, Erwan Sulaiman, Hassan Ali Soomro, Faisal Amin, Laili Iwani Jusoh, Enwelum I Mbadiwe
[1]Research Center for Applied Electromagnetics (EMCenter), Universiti Tun Hussein Onn Malaysia (UTHM), 86400 Parit Raja, Johor, Malaysia

Article Info	ABSTRACT

Recently, a three-phase Field Excitation Flux Switching Motor (FEFSM) using salient rotor has been introduced, suitable for high torque, high power as well as high speed diverse performances due to their advantages of easy rotor temperature elimination and controllable field excitation (FE) flux. However, existing FEFSMs are found to have low torque performance as the salient rotor structure has caused longer flux path, and consequently weak flux linkage. Therefore, a new structure of a single-phase FEFSM using segmental rotor and non-overlap windings is proposed. There are two valuable findings found in this topology, first is less copper loss due to the non-overlap windings between armature and FE coils, and secondly the segmental rotor structure has produces shorter flux path to produce high torque, less rotor weight as well as robust rotor at high speed condition. Flux linkage, back-emf, average torque and output power characteristics of the initial and optimized designs have been investigated and compared using 2D Finite Element Analysis (2D-FEA) through JMAG Designer version 15. Based on the 2D-FEA analysis, the average torque has increased by 81.3% to 1.65 Nm, while the output power of 466.5 W, increased of 68.2%. In conclusions, a FEFSM using segmental rotor and non-overlap windings is considered as the best single-phase motor due to their optimal performances and less copper loss.

Corresponding Author:

Mohd Fairoz Omar,
Research Center for Applied Electromagnetics (EMCenter),
Universiti Tun Hussein Onn Malaysia (UTHM),
86400 Parit Raja, Johor, Malaysia.
Email: fairoz.omar@yahoo.com

1. INTRODUCTION

The first concept of flux switching machine (FSM) was founded and published in 1950. FSM consists of all flux sources in the stator. Besides the advantage of brushless machines, FSM has a single piece of iron rotor structure allowing to be apply in robust and high-speed applications [1]. Over the past ten years, many new FSM topologies have been developed for various applications, ranging from low-cost domestic appliances, automotive, wind power, aerospace, and others [2], [3].

Figure 1 illustrates the basic operation of FSM. Considering Figure 1(a), the excitation of the field and armature windings at positive current creates a flux vector in the north-westerly direction and north-easterly direction, respectively. The combined flux generated by the two coils caused a flux moving vertically upwards and the rotor aligned itself with a pair of vertical stator. Additionally, Figure 1(b) illustrates the current in the armature winding is reversed, while the FEC winding continues being excited in the same direction by the effect of the 180° flux shifting from west-south [4].
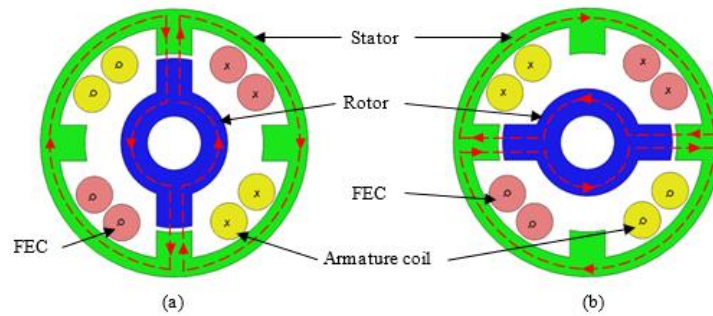
Figure 1. Operating principle of FEFSMs

The result from the 180° shifting makes the rotor tends to align with the stator poles based on the flux movement in a westerly direction through horizontal stator poles. Therefore, each reversal of current directions in the armature causes the stator flux vector to switch between horizontal and vertical directions, hence introducing the name FSM [5].

Generally, FSM can be categorised into three groups: permanent magnet flux switching motor (PMFSM), field excitation flux switching motor (FEFSM), and hybrid excitation flux switching motor (HEFSM). PMFSM and FEFSM using PM and field excitation coil (FEC), respectively, as their main flux sources, while HEFSM combines both PM and FEC as its main flux source. Compared to these three types of FSM, FEFSM has shown significant advantages due to low manufacturing cost, and demagnetization can be neglected because of FEFSM is magnet-less machine. In addition, the magnetic field produced by the FECs can be controlled allowing FEFSM suitable to be utilized on various equipments [6]-[8].

Figure 2 shows the example of three-phase and single-phase salient rotor FSM with overlap windings configurations. The author [9] introduced a new structure of three-phase 24S-10P FEFSM with overlapping windings between 12 armature coils and 12 FEC coils as illustrated in Figure 2(a). With a single polarity of the FEC winding, the motor becomes easy to construct, and produces less flux leakage. This motor is suitable for industrial applications which require high torque and power capability [10], [11]. This is because of its high torque and power of 240.5 Nm and 25.7 kW, respectively at base speed of 1,200 rpm.

Figure 2(b) shows the single-phase salient rotor 12S-6P FEFSM. The proposed motor is introduce in order to solve the problem of high cost consumption in PMFSMs technology [12]. The stack length and stator outer diameter are set to 25 mm and 90 mm, respectively. This motor has 12 slots, in which 8 slots accommodate 4 non-overlap FECs and each slot from the remaining 4 slots is divided into 2 to form 4 overlap armature coils. Consequently, the motor has shorter end windings, and better copper usage.
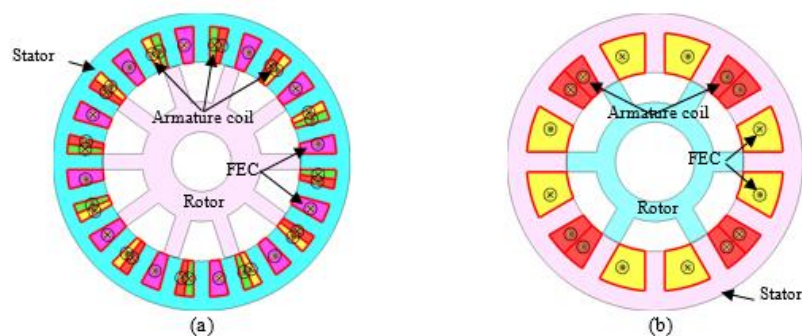

Figure 2. FEFSM with salient rotor (a) 3-phase 24S-10P and (b) Single-phase 12S-6P

However, the salient rotor structure of existing FEFSM produces longer flux path, higher rotor volume, and increase the rate of iron loss. In addition, the overlap winding technique applied between armature coils and FECs has produced high volume of motor and reduce low torque density. Besides, high copper wire consumption has produced high copper loss and reduces the efficiency.

This paper presents a new single-phase segmental rotor 12S-6P FEFSM with non-overlap windings. The proposed motor has 12 slots for armature coils winding, 12 slots for FECs winding and 6 segmental rotors

that provide a short flux path from the stator to the rotor and vice versa. Consequently, the proposed motor enables higher flux yields and increases the output torque. 2D-Finite Element Analysis (FEA) through JMAG Designer version 15 is used to investigate the coil test, flux linkage, flux line, back-emf, average torque and output power characteristics of the proposed motor.

2. DESIGN RESTRICTIONS AND SPECIFICATIONS OF THE INITIAL DESIGNED

The initial design restriction is illustrated in Table 1 and Figure 3 demonstrates the structure of single-phase segmental rotor 12S-6P FEFSM with non-overlap windings. The maximum of armature current density, J_A and field excitation current density, J_E are set to 30 A_{rms}/mm^2 and 30 A/mm^2, respectively. The electrical silicon steel 35A250 material is used for stator and rotor body. While, stator outer diameter, rotor outer diameter, shaft diameter and air gap are restricted to 75 mm, 45 mm, 30 mm and 0.5 mm, respectively. The single rotor structure with stack length of 20.3 mm is mechanically robust because it consists only of stacked electromagnetic sheets.

Table 1. Design Restriction and Specifications of the Initial Design

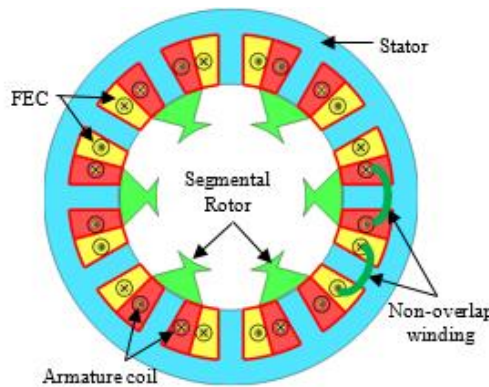| Parameter	Value	Unit
Maximum DC current	7.5	A
Maximum armature current	10.5	A
Maximum J_A	30	A_{rms}/mm^2
Maximum J_E	30	A/mm^2
Stator outer diameter	75	mm
Rotor outer diameter	45	mm
Stack length	20.3	mm
Air gap	0.25	mm
Shaft diameter	30	mm
Number of FEC turn	93	turn
Number of armature turn	93	turn

Figure 3. Initial structure of the proposed FEFSM

3. PERFORMANCES OF INITIAL DESIGN OF FEFSM
3.1. Coil test

Result of the proposed single-phase 12S-6P FEFSM using segmental rotor coil test is depicted in Figure 4, at the point when J_A and J_E are set to maximum of 30 A_{rms}/mm^2 and 30 A/mm^2, respectively and rotor is shifted by 45° mechanical. Clearly, the flux linkage at highest J_A is 0.0718 Wb, 39.4% higher than magnetic flux at maximum J_E. However, the magnetic flux profile shows unbalance flux between positive and negative cycles due to flux leakage occurs at 230° to 310° electric when flux attempt to flow from stator to rotor. Besides, the flux linkage of J_E only is slightly lower than flux linkage of J_A due to magnetic flux generated from FEC will move around the stator and rotor before reaching the armature windings. The flux linkage of FEC lead 90°

of armature coil flux linkage, hence ensuring the motor to be worked based on standard operating principle of single-phase motor.

3.2. Result of Flux Line

Figure 5 delineates the flux line delivered under maximum J_E of 30 A/mm² at 0° or 360°, 90°, 180°, and 270° electric cycle. Figure 5 (a) and (c) demonstrate the magnetic field streams from the stator to the rotor and back to stator seem shorter at all armature coils to form one complete magnetic flux cycle. Besides, the flux line profile also indicates the highest flux linkage achieved is at 180°, proven through flux characteristics at coil test as illustrated in Figure 4. Concentrated flux is highlighted with red circles in Figure 5 (b) and (d) because flux does not legitimately flow to form one complete cycle due to incomplete magnetic flux paths that connects the adjacent stator teeth. In addition, the flux line also proved the condition of zero rotor position in which the magnetic flux is zero when the rotor positions at 90° and 270°.
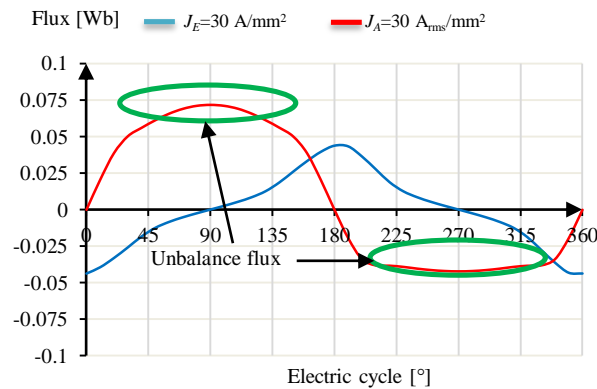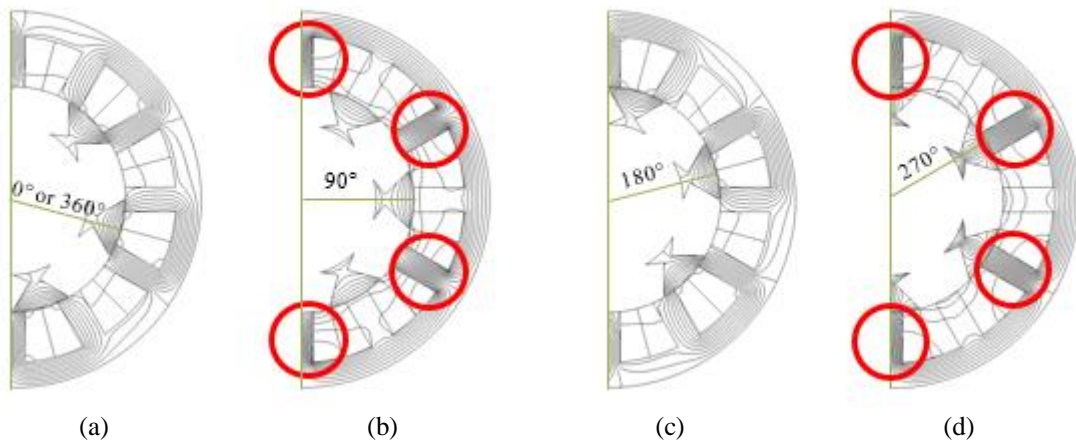
Figure 4. Flux linkage in open-circuit test

Figure 5. FEC flux line at 4 electric cycle positions, (a) 0° or 360°, (b) 90°, (c) 180° and (d) 270°

3.3. Result of Back-emf

Figure 6 shows back-emf of the proposed single-phase 12S-6P FEFSM. The highest amplitude of back-emf is 13.4 V. From the figure the back-emf has high distortion between 45° to 135° and 215° to 335° electric cycle due to high 3rd and 5th of total harmonic distortion (THD). In addition, the unsmooth sinusoidal of J_E flux linkage as illustrated in Figure 4 also led to high THD.
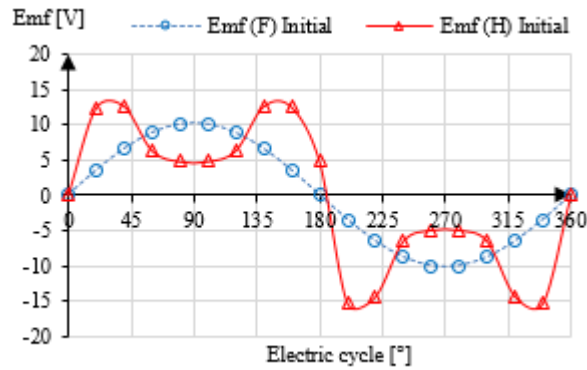
Figure 6. Back-emf of the proposed single-phase 12S-6P FEFSM

3.4. Initial Performances of Torque and Power

The initial design has produced torque and power of 0.91 Nm and 277.5 W, respectively at based speed of 2,899 rpm. The performance of torque and power decreased proportionally with increase of speed, which is at medium speed region of 4,000 rpm, the torque produced is 0.65 Nm and the power achieved is 269 W. While at high speed region of 8,000 rpm, the torque produced is 0.27 Nm and the equivalent power obtained is 245 W.

4. 12S-6P FEFSM IN DESIGN OPTIMIZATION

In order to improve the performance of torque and power, the optimization process is carried out by using deterministic optimization technique. The deterministic optimization technique is also expected to solve the problem of back-emf disruption, unbalanced flux of armature current only and unsmooth FE flux linkage.

Figure 7 shows the procedures of deterministic optimization method. From the figure, each optimization cycle is divided into 3 stages namely rotor, armature slot and FEC slot. To determine whether the optimization process is achieved or not, the determination process is performed by comparing the torque optimized, Topt at the end of each cycle with the torque performance of the previous cycle, Tci. Generally, there are seven parameters involved in the optimization process: R_1, R_2, R_3, A_1, A_2, F_1, and F_2 as illustrated in Figure 8. In addition, it should be noted in the optimization process, the following parameters need to be maintained as initial parameter: outer radius of stator (S_o), armature and field excitation number of turns (N_A and N_E), air gap (A_g) and current input of armature and field excitation (I_A and I_E).Table 2 illustrates the comparison between initial and optimized design specifications. Obviously, parameters such as S_o and A_g are maintained, while ratio between the rotor outer radius, R_1 and the stator outer radius, S_o decreased from 0.59 to 0.56. From the table, parameters A_1 and F_1 have increased, while parameters of A_2 and F_2 have decreased due to the 93 number of turns for both slots are remains unchanged until the highest torque value is achieved. In addition, segmental rotor span, R_2 shows the highest change of 66.7% from 15 degrees to 25 degrees. This proves that the use of segmental rotor has influenced the flux linkage interaction between stator and rotor.

4.1. Result of J_E and J_A Flux Linkage

Figure 9 shows the flux linkage comparison between initial and optimized designs of single-phase FEFSM using segmental rotor. Clearly, the flux linkage profile at maximum J_E is more sinusoidal and increases by 64% from 0.0435 Wb to 0.0714 Wb. While, the flux linkage at maximum J_A shows a more balance than the initial design because of the ratio between positive and negative amplitudes has been reduced by 32.3% from 1.7 to 1.15. In addition, the maximum flux linkage for J_A is 0.11 Wb, 35.5% higher than the flux linkage at maximum J_E.

Figure 9 shows the flux linkage comparison between initial and optimized designs of single-phase FEFSM using segmental rotor. Clearly, the flux linkage profile at maximum J_E is more sinusoidal and increases by 64% from 0.0435 Wb to 0.0714 Wb. While, the flux linkage at maximum J_A shows a more balance than the initial design because of the ratio between positive and negative amplitudes has been reduced by 32.3% from 1.7 to 1.15. In addition, the maximum flux linkage for J_A is 0.11 Wb, 35.5% higher than the flux linkage at maximum J_E.
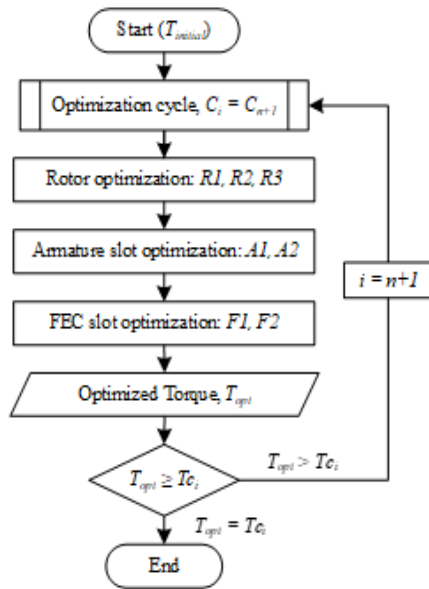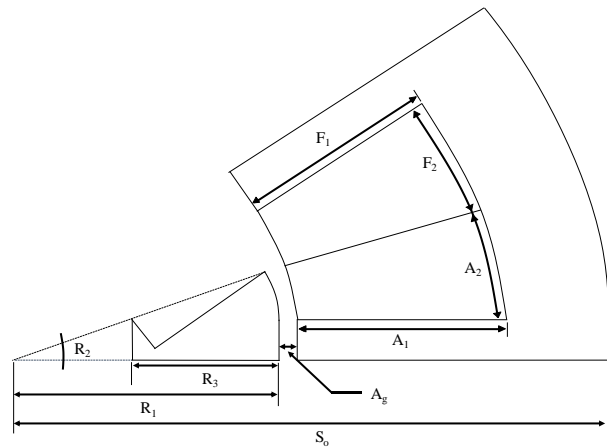
Figure 7. Optimization process

Figure 8. Parameter sensitivities in optimization processes

4.2. Result of Back-emf

The back-emf result of both designs is illustrated in Figure 10. Both back-emf readings are taken when the speed is set at 500 rpm. From the figure, the highest amplitude of the back-emf after optimization is 24.9 V and shows an increase of 85.7% from the initial design amplitude. This happens because of J_E flux linkage is increased. However, the back-emf profile shows a lot of improvement, especially distortion in harmonic number 3 and 5 have decreased by 78.5% and 84.4%, respectively as illustrated in Figure 11.
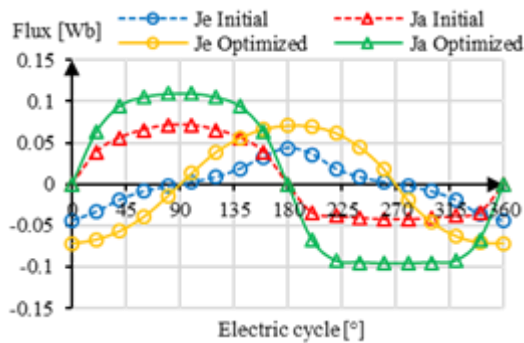

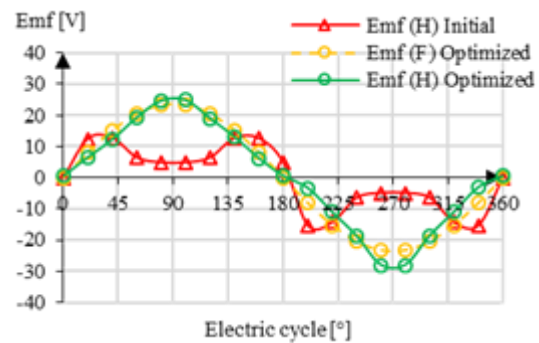Figure 9. Flux linkage of 12S-6P FEFSM

Figure 10. Back-emf of optimization 12S-6P FEFSM

4.3. Flux Distribution

Figure 12 shows flux distribution when the motor is given the maximum armature current, I_A and rotor at 270° electric cycle. From Figure 12(a), the flux distribution of initial design indicates a lot of flux leakage on each side of armature coil tooth. This happens because of segmental rotor span is not sufficiently large has caused flux from stator to rotor unable to flow and leak out from the flux path. Figure 12(b) shows the flux distribution after the optimization process is performed. The larger segmental rotor span allows flux to flow between two stator teeth and one segmental rotor and reduce flux leakage and enhance flux concentration. It also proved the result of flux linkage as shown in Figure 9 is acceptable, which is the issue of unbalanced flux has been solved due to the ratio between positive and negative amplitudes of armature flux has been reduced.

Table 2. Design Specifications of the Initial and Optimized Design

| Parameter	Abb.	Initial	Opt.	Unit
Rotor outer radius	R1	22.25	21.25	mm
Segmental rotor Span	R2	15	25	mm
Segmental rotor high	R3	7.25	7.25	mm
Segmental Rotor inner radius	Ri	15	14	degree
Stator outer radius	So	37.5	37.5	mm
Stator inner radius	Si	22.5	21.5	mm
Armature slot high	A1	10	10.4	mm
Armature slot width	A2	8.65	8.35	mm
FEC slot high	F1	10	11.4	mm
FEC slot width	F2	8.65	8.61	mm
Air gap	Ag	0.25	0.25	mm
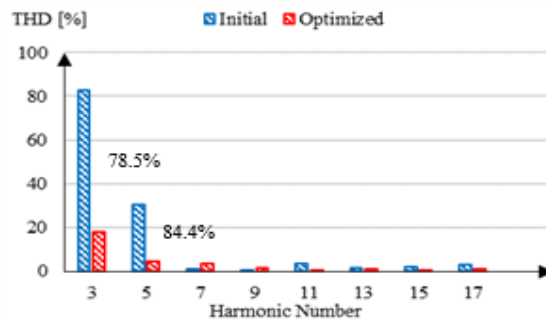
Figure 11. THD versus harmonic number
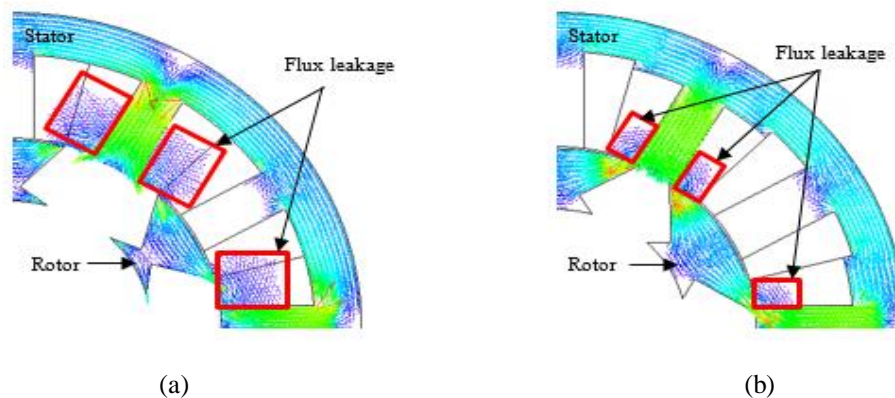

(a)   (b)

Figure 12. Flux distribution of single-phase FEFSM, (a) initial design, and (b) optimized design

4.4. Various Torque at Various J_E and J_A

Figure 13 shows various torque capability of the proposed single-phase 12S-6P FEFSM using segmental rotor. From the figure, the torque has increased steadily with the increase of J_A and J_E. The torque of optimized design has increased by 80.8% from 0.91 Nm to 1.65 Nm, achieved when maximum J_A and J_E. At the maximum J_E of 30 A/mm^2, while JA are set to 10 A$_{rms}$/mm^2 and 20 A$_{rms}$/mm^2, the torque obtained are 0.74 Nm and 1.32 Nm, respectively.

4.5. Torque and Power versus Speed Characteristics

The torque and power versus speed characteristics of the initial and optimized design of single-phase FEFSM using segmental rotor are plotted in Figure 14. From the figure, the optimized design has produced highest torque and power of 1.65 Nm and 466.5 W, respectively. Furthermore, the highest constant torque starts to decrease when the speed exceeds of 2,304 rpm. The motor power increases up to a maximum and start to decline when reaching the speed of 4,500 rpm with the corresponding torque of 0.99 Nm. In addition, at high speed region of 8,000 rpm, torque and power performances are 0.5 Nm and 418.9 W, respectively.

Therefore, the proposed motor is considered suitable for single-phase applications requiring low torque and high speed. In short, the optimized design has succeeded in increasing torque and power to optimal performances of 81.3% and 68.2%, respectively.
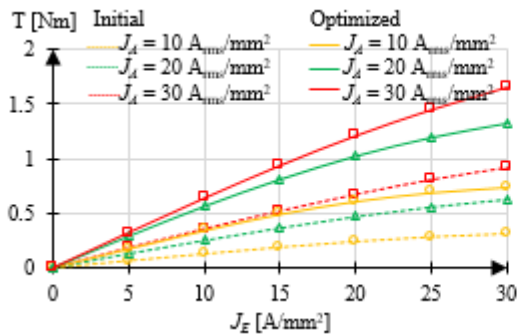

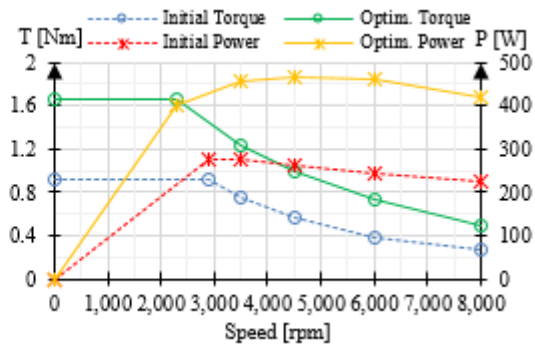Figure 13. Torque versus J_E at various J_A

Figure 14. Torque and power versus speed

5.   CONCLUSION

In this paper, design studies, optimization and performance analysis of single-phase 12S-6P FEFSM using segmental rotor and non-overlap windings is presented. The initial and optimized design are clearly demonstrated. Implementation of optimization using a deterministic approach to the proposed motor for optimum performances has been presented and clearly analysed. As a conclusion, the torque and power of the optimum design single-phase 12S-6P FEFSM using segmental rotor and non-overlap windings has been increased approximately by 81.3% and 68.2%, respectively compared to the initial design.

REFERENCES

[1]   M. M. a Mazlan, E. Sulaiman, and T. Kosaka, "Design study of single phase outer-rotor hybrid excitation flux switching motor for hybrid electric vehicles," *Proc. 2014 IEEE 8th Int. Power Eng. Optim. Conf. PEOCO* 2014, no. c, pp. 138–143, 2014.
[2]   E. Sulaiman, "Design Studies on Less Rare-Earth and High Power Density Flux Switching Motors with Hybrid Excitation/Wound Field Excitation for HEV Drives," 2012.
[3]   H. Pollock, C. Pollock, R. T. Walter, and B. V. Gorti, "Low cost, high power density, flux switching machines and drives for power tools," *IAS Annual Meeting on Conference Record of the Industry Applications Conference*, 2003, pp. 1451–1457.
[4]   C. Pollock and M. Wallace, "The flux switching motor, a DC motor without magnets or brushes," *Conf. Rec. 1999 IEEE Ind. Appl. Conf. 34th IAS Annu. Meet.*, vol. 3, pp. 1980–1987, 1999.
[5]   M. Jenal, S. A. Hamzah, F. Khan, H. A. Soomro, and E. Sulaiman, "Performance investigations of flux switching machines for light weight electric vehicles," *IEEE Conf. Energy Conversion, CENCON 2015*, pp. 78–83, 2016.
[6]   C. Yu, S. Niu, S. L. Ho, and W. N. Fu, "Magnetic Circuit Analysis for a Magnetless Double-Rotor Flux Switching Motor," *IEEE Trans. Magn.*, vol. 51, no. 11, pp. 1–4, 2015.
[7]   S. M. Yang, J. H. Zhang, and J. Y. Jiang, "Modeling Torque Characteristics and Maximum Torque Control of a Three-Phase, DC-Excited Flux-Switching Machine," *IEEE Trans. Magn.*, vol. 52, no. 7, pp. 7–10, 2016.
[8]   H. Q. Nguyen, J. Y. Jiang, and S. M. Yang, "Design of a 12-slot 7-pole wound-field flux switching motor for traction applications," *in IEEE International Conference on Industrial Technology (ICIT)*, 2016, pp. 1275–1280.
[9]   E. Sulaiman, M. F. M. Teridi, Z. A. Husin, M. Z. Ahmad, and T. Kosaka, "Performance comparison of 24S-10P and 24S-14P field excitation flux switching machine with single DC-Coil polarity," *in Proceedings of the 2013 IEEE 7th International Power Engineering and Optimization Conference, PEOCO*, 2013, vol. 1, pp. 46–51.
[10] P. Su, W. Hua, G. Zhang, and M. Cheng, "Investigation of a novel rotor permanent magnet flux switching machine for EV and HEV applications," *2015 IEEE Int. Magn. Conf. INTERMAG 2015*, vol. 50, no. 11, p. 8102405, 2015.

[11] Y. L. Karnavas, I. D. Chasiotis, and E. D. Peponakis, "Optimization of Standard PMDC Motors used in Automotive Applications for Óigher Power Density," in *Third International Conference on Mathematics and Computers in Sciences and in Industry (MCSI)*, 2016, pp. 7–13.

[12] Y. J. Zhou and Z. Q. Zhu, "Comparison of low-cost single-phase wound-field switched-flux machines," *IEEE Trans. Ind. Appl.*, vol. 50, no. 5, pp. 3335–3345, 2014.

BIOGRAPHIES OF AUTHORS

	Mohd. Fairoz Omar was born in Johor, Malaysia, on May 12, 1986. He received Diploma in Electric and Electronic Engineering from Politeknik Ibrahim Sultan in 2008. Since October 2008, he has been working under Asian Geos (M) Sdn. Bhd as Technician. He received his B.E Degree in Electronic Engineering and M.E Degree in Electrical Engineering from University Tun Hussein Onn Malaysia, in 2014 and 2016, respectively. Currently, he is Ph.D. Degree at Department of Electrical Power Engineering, University Tun Hussein Onn Malaysia. His research interests include single-phase field excitation flux switching machines (FEFSMs) for lightweight applications.
	Erwan Sulaiman was born in Johor, Malaysia, on August 31, 1978. He received his B.E and M.E Degrees in Electrical Engineering from University of Malaya in 2001 and University Tun Hussein Onn Malaysia (UTHM) in 2004. He has been with UTHM from December 2004 as a lecturer. He received Doctor Degree in Electrical Engineering from Nagoya Institute of Technology (NIT), Japan in 2012. He is currently senior lecturer at Department of Electrical Power Engineering, University Tun Hussein Onn Malaysia. His research interests include design optimizations of HEFSM, FEFSM, PMFSM, in particular, for HEV drive applications.
	Hassan A. Soomro was born in Nawabshah, Sindh, Pakistan, on May 01, 1985. He received his B.E and M.E degrees in Electrical Engineering from Quaid-e-Awam University of Engineering Science and Technology Nawabshah, Pakistan in 2008 and University Tun Hussein Onn Malaysia (UTHM) in 2016 respectively. He has been with UTHM from April 2014 as Graduate Assistant researcher. Currently, He is doing PhD in Department of Electrical Power Engineering, University Tun Hussein Onn Malaysia. His research interests include design and optimizations HEFSM with segmental rotor structure, In particular, for aircraft applications.
	F. Amin Faisal Amin got his Intermediate degree in Pre-Engineering from D.J. Sindh Govt. Science College, Pakistan in 2010, then he was awarded Bachelor of Electrical Engineering degree from Sir Syed University, Pakistan. Now he got enrolled in Universiti Tun Hussein Onn Malaysia for completion of Master of Engineering degree.
	Laili Iwani binti Jusoh was born in Besut, Terengganu on August 2, 1987. She received her B.E (2007-2010) and M.E (2010-2014) degrees in Electrical Engineering from University of Tun Hussein Onn, Malaysia. Since September 2015, she has been a researcher in Research Center for Applied Electromagnetics (EMC) at Universiti Tun Hussein Onn, Johor, Malaysia. Her research interest are mainly focused on Design and Investigation of Single Phase Permanent Magnet Flux Switching Machines (PMFSM) for Electric Bicycle Application.